

Self-Amplified Spontaneous Emission and Bunching at 3 GHz in a Microwave Free-Electron Laser

T. Lefevre, J. Gardelle, G. Marchese, and J.L. Rullier

CEA/Centre d'Etudes Scientifiques et Techniques d'Aquitaine, BP 2, 33114 Le Barp, France

J. T. Donohue

Centre d'Etudes Nucléaires de Bordeaux-Gradignan, BP 120, 33175 Gradignan, France

(Received 23 July 1998)

The CEA/CESTA free-electron laser amplifier has been operated in the self-amplified spontaneous emission mode. This waveguide laser has two resonant frequencies for given beam energy and wiggler field, at approximately 3 and 35 GHz, respectively, for our operating conditions. Highly reproducible microwave power levels of 40 MW and pronounced electron bunching are seen at the lower frequency. Streak camera photographs of the time dependence of the bunching mechanism at the lower frequency are presented. The bunching is accompanied by a significant loss of electrons from the beam. [S0031-9007(98)08180-0]

PACS numbers: 41.60.Cr, 52.75.Ms

The free-electron laser (FEL) community has recently become interested in the phenomenon called self-amplified spontaneous emission (SASE) [1], and several groups have reported new experimental results [2–4]. A reason for this is the possibility of obtaining intense sources of far ultraviolet or x rays by using GeV energy electron beams in a SASE FEL [5,6]. The subject is discussed by Freund and Antonsen [7], who note that the term super-radiance was used to describe intense spontaneous emission seen in low energy single-pass FELs. These FELs use a pulse of electrons whose duration is much greater than the period of the radiation emitted. FEL operation at millimetric [8] and far-infrared [9] wavelengths has been reported in this super-radiant mode. The new interest concerns FELs driven by radio-frequency (rf) accelerators, in which the electron beam has both a macropulse structure (corresponding to the pulsing of the accelerator) and a micropulse structure, corresponding to the window in the accelerator rf cycle [2–4]. Theoretical work on SASE may be traced back to the early days of FEL [10–13], and a thorough discussion of super-radiance in high-gain FELs is given in the review article of Bonifacio and co-workers [14]. They point out that a key parameter in super-radiance is slippage, which may be defined as $v_g/v_z - 1$, where v_g and v_z denote the group velocity of the radiation and the mean axial velocity of the electrons, respectively. Our results were obtained in a waveguide which has two FEL resonant frequencies [7], and they concern mainly the lower frequency for which v_g is much less than v_z . The corresponding slippage parameter is approximately 0.7, and previous experiments have not operated in such a regime.

Although the observation of high power output from a FEL indicates that bunching has occurred, optical measurement of it has been performed only recently. With our FEL operating in the amplifier mode, direct optical observation of electron bunching at 35 GHz was made [15]. In an at-

tempt to increase the current and improve the bunching, a second run with a larger radius beam tube in the wiggler was made, and while better bunching at 35 GHz was found, a strong signal near 3 GHz was also observed [16]. This radiation is at the second resonant FEL frequency. Inasmuch as this signal was not injected, it may be called SASE, but the simultaneous presence of the strongly amplified input signal at 35 GHz prevents us from making such a straightforward interpretation. Given the importance of understanding the bunching mechanism in SASE, we have made a long series of shots with our FEL in the SASE mode (i.e., no injected signal). The optical data reveal in detail the bunching, and we then study its variation as a function both of length in the wiggler and time in the beam pulse.

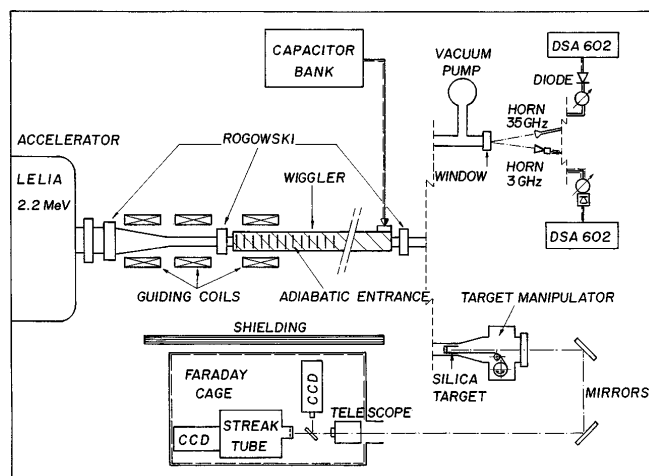


FIG. 1. The experimental layout with, at right, two distinct detector configurations. At the top are shown the horns and lines for measuring output power and frequency, while below are shown the beam position camera and the streak camera for observing bunching.

In this paper we concentrate on the 3 GHz signal, since it is much stronger and far more reproducible than the 35 GHz signal, which has a large bandwidth (≈ 5 GHz). The empty waveguide cutoff frequency is 2.88 GHz, and if the usual corrections for the plasma frequency are applied, the resonant frequencies for our beam energy spread and typical wiggler fields lie in the interval 2.98–3.08 GHz. Since our signal lasts about 25 ns, the minimal uncertainty in frequency is 40 MHz. Consequently, the frequency of this signal is, within this uncertainty, quite stable.

A schematic of our experiment is shown in Fig. 1. The induction linac LELIA [17] delivers a 800 A electron beam of energy 2.2 MeV, which is transported into a helical wiggler. There are 26 periods of 12 cm, including a six period adiabatic entrance.

On the right-hand side of the Fig. 1 we show two distinct setups, the upper for observing rf power at both frequencies, the lower for performing optical measurements of beam position (with the gated camera) and bunching (with the streak camera). Frequency measurements were made using heterodyne methods for the upper frequency and direct signal analysis with a fast oscilloscope for the lower. In order to study output power as a function of

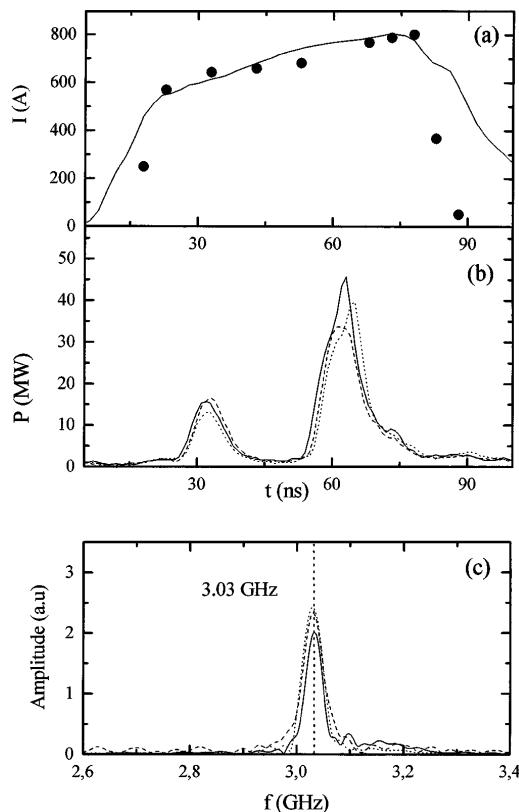


FIG. 2. (a) The beam current at the wiggler entrance (solid curve) vs time together with integrated beam intensities seen by the camera at period 15 using a 5 ns exposure time (circles). (b) Reproducibility of the output power in the 3 GHz horn as a function of time in the pulse. (c) Fourier analysis of the 3 GHz horn signal for three different shots.

axial distance, a movable permanent magnet was used to deflect the electron beam into the beam pipe at any desired position. The bunching of the electrons was observed by causing the beam to strike a 2-mm-thick fused silica target, producing Cerenkov radiation. The target could be moved under vacuum, allowing us to observe bunching at any position. By varying the trigger delays of the cameras we could study the bunching as a function of time.

In Fig. 2a we show the beam current, as measured at the wiggler entry (solid curve), and the light intensities (circles) as observed with the gated camera when the target is placed at period 15 of the wiggler, both as a function of time. We have arbitrarily normalized the latter to agree with the maximum of the former, and we observe fair agreement between these two measurements, both of which indicate that the bulk of the current pulse lasts 60 ns. Figure 2b shows output power as a function of time as detected with the low-frequency horn and using the full length of the wiggler. Three different shots are shown, and the two-peaked behavior seen is typical of all of our shots. The bunching measurements also display this two-peaked structure. The maximum rf power at 3 GHz was 40 ± 10 MW, which is somewhat less than what we observed previously in the amplifier mode. At the upper frequency, the output power was limited to a few MW. Measurements of the intensity made using varying lengths indicate that for neither frequency has saturation occurred. Finally in Fig. 2c we show the Fourier analysis of the low-frequency horn signal for three shots, in the region near 3 GHz. Again a high degree of reproducibility is seen. On

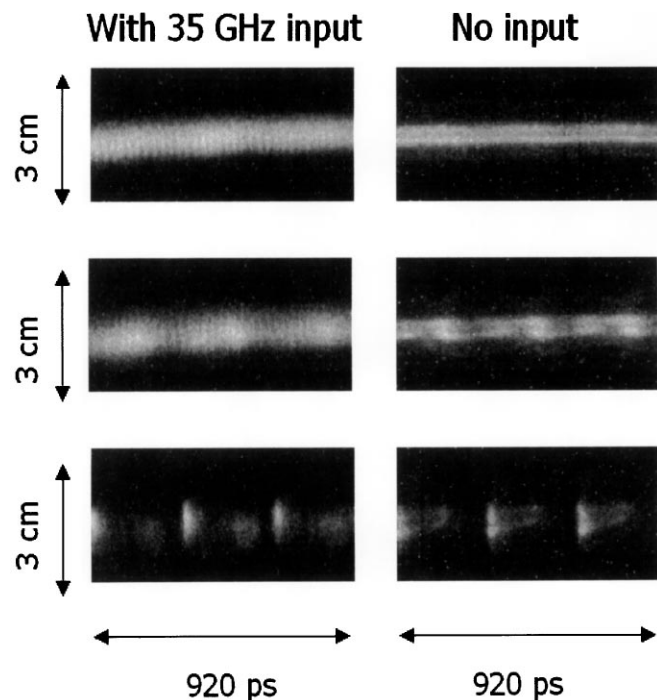


FIG. 3. Streak camera photographs of bunching when the FEL is running in the amplifier mode (left) and the SASE mode (right), for three different values of time in the beam pulse.

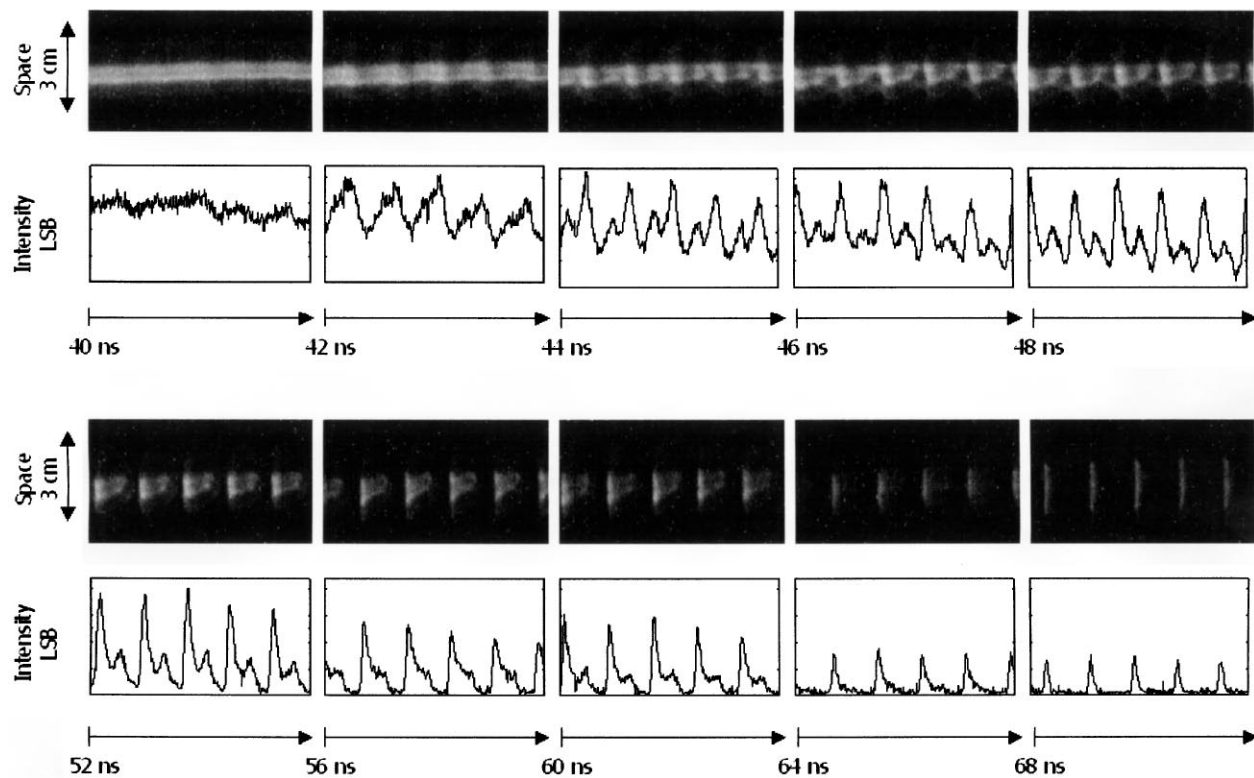


FIG. 4. Streak camera photographs and their digitized representations, as observed at wiggler period 23, for ten different times in the beam pulse and a 1.66 ns time interval.

the basis of this stability, we feel justified in treating on the same footing data from different shots.

In Fig. 3 we show a comparison between our previous measurement of bunching in the amplifier mode (at 35 GHz, left) and the SASE measurements (right). The time interval between two photographs is 6 ns. In the amplifier mode, and for early times, the bunching at 35 GHz is clear, and the bunching at 3 GHz is barely visible under it. Towards the end of the amplifier mode pulse, the bunching at 35 GHz has disappeared, and the signal strongly resembles the corresponding SASE signal. In fact, if one ignores the presence of the 35 GHz bunching in the photographs, the 3 GHz bunching is quite similar in both cases. On the basis of these images, we suggest that the mechanism of generation of the 3 GHz bunching is independent of the presence of an appreciable signal at 35 GHz. However, the difference in output powers suggests that there may still be some cooperative effects between the two frequencies.

A sequence of streak camera images, taken at period 23 in the wiggler, and for various time slices in the beam pulse is displayed in Fig. 4. Below each photograph appears the corresponding beam current profile as a function of time during 1.66 ns. As can be seen by following the frames, the low-frequency bunching, weak in the first frame, grows with time until a large fraction of the current is confined to a short time interval. Two important aspects of these images are the substantial transverse widening of the beam

from early to late times, easily seen by comparing the first and last frames, as well as the fact that the bunch images in frames 3–5 are slightly skewed from the vertical. We also see that electrons are being lost as the bunching sharpens with time. However, this loss of current is not in conflict with the measurements shown in Fig. 2a, since they were made either at the wiggler entrance or far enough upstream that bunching was insignificant. We note that this loss of electrons is not reproduced by our numerical simulations using the stationary amplifier code SOLITUDE [18] in which the input power level is adjusted to yield comparable output power at 3 GHz. We have performed similar but less thorough analyses at several different target positions, and the time dependence of bunching we observe is similar to that shown here, even for such early periods as 17, where the output power is only of the order of 10 kW. However, the bunching happens at increasingly later times as one moves upstream. From these observations we conclude that at a fixed position, the transition from a uniform to a bunched beam occurs in a short time, 2–3 ns, and is then followed by a slow but steady loss of current.

In these photographs and the current profiles one begins with a relatively unbunched beam in frame 1, next one observes bunching at the fundamental frequency (i.e., 3 GHz) in frame 2, then one sees second and higher harmonics as the frame numbers increase. To illustrate this, we show in Fig. 5 the results of a fast Fourier transform of the digitized signals shown in the previous

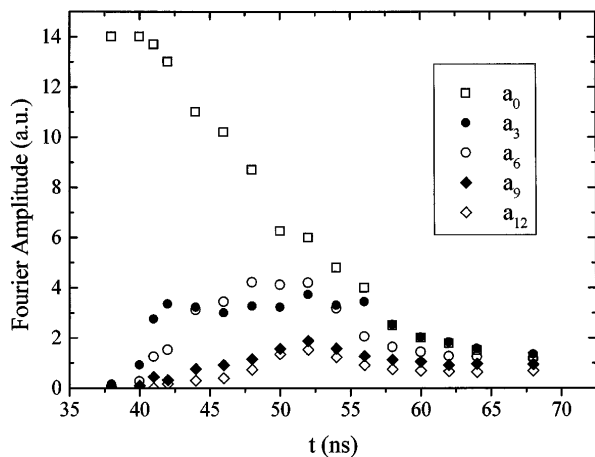


FIG. 5. The first five coefficients, denoted a_0 , a_3 , a_6 , a_9 , and a_{12} , of the fast Fourier transform of the digitized representations shown in the preceding Fig. 4, as functions of time in pulse.

figure. The total current is represented by a_0 , while the coefficients at (approximately) 3, 6, 9, and 12 GHz are denoted as a_3 , a_6 , a_9 , and a_{12} , respectively. A striking feature is the quasilinear fall of the total current. In contrast to the behavior of a_0 , the coefficient a_3 increases from noise to a practically constant value for the duration of the pulse. This rapid rise of a_3 is responsible for the transition from an unbunched to a bunched beam. The coefficient a_6 appears only slightly later than a_3 and it takes on even greater values. We propose a tentative explanation for this behavior. If the usual FEL resonant condition is satisfied, then there are two values, separated by π , of the ponderomotive phase $(k + k_w)z - \omega t$ for which the electric field and the electron's transverse velocity are orthogonal. Electrons with these phases neither gain nor lose energy, and one may refer to these phases as fixed points. Nearby electrons are attracted towards the stable fixed point, while they are repelled by the unstable one. Thus the unstable fixed point will be a local maximum in a region where the density is decreasing. The resulting beam profile will thus have a substantial second harmonic. In the final frames, where the current has decreased substantially, the bunches appear almost as a sequence of Dirac-delta functions. Noting that in our experiment, the slippage is both large and negative, and the frequency is very close to cutoff, we can suggest that some combination of these effects might be the cause of this loss, and more experiments are necessary to understand the phenomenon. It is interesting to note that Barletta and collaborators [19] have generated current distributions resembling ours, although the beam energy and output power level are quite different.

In conclusion, we have observed a highly reproducible SASE mechanism, responsible for high microwave power

output (≈ 40 MW) and sharp electron bunching at the lower resonant frequency of our pulsed FEL. In comparison with our previous observation of bunching at 3 GHz when running in the amplifier mode at 35 GHz, the bunching we observe here is uncontaminated by interference from the upper frequency, and a detailed study of its time dependence has been presented. We observed that significant bunching can occur without high output power, and that very sharp bunching is accompanied by an important loss of electrons. We remark that we have found no evidence for a coupling between the two resonant FEL frequencies, of the sort proposed by Piovella *et al.* [20].

We thank D. Gogny for his advice and encouragement, M. Lavergne, C. Vermare, and D. Villate for their help with the optical measurements, and Marc Padois for his conscientious operation of the accelerator.

- [1] K.-J. Kim, Nucl. Instrum. Methods Phys. Res., Sect. A **393**, 147 (1997).
- [2] R. Prazères *et al.*, Phys. Rev. Lett. **78**, 2124 (1997).
- [3] M. Hogan *et al.*, Phys. Rev. Lett. **80**, 289 (1998).
- [4] D. Bocek *et al.*, Nucl. Instrum. Methods Phys. Res., Sect. A **375**, 13 (1996).
- [5] R. Thatchin *et al.*, Nucl. Instrum. Methods Phys. Res., Sect. A **375**, 27 (1996).
- [6] J. Rossbach *et al.*, Nucl. Instrum. Methods Phys. Res., Sect. A **375**, 269 (1996).
- [7] H.P. Freund and T.M. Antonsen, *Principles of Free-electron Lasers* (Chapman and Hall, London, 1996).
- [8] T. Orzechowski *et al.*, Nucl. Instrum. Methods Phys. Res., Sect. A **250**, 144 (1986).
- [9] D. Kirkpatrick *et al.*, Nucl. Instrum. Methods Phys. Res., Sect. A **285**, 43 (1989).
- [10] J.B. Murphy and C. Pellegrini, Nucl. Instrum. Methods Phys. Res., Sect. A **237**, 159 (1985).
- [11] R. Bonifacio, C. Pellegrini, and L. Narducci, Opt. Commun. **50**, 373 (1984).
- [12] Ya.S. Derbenev, A.M. Kondratenko, and E.L. Saldin, Nucl. Instrum. Methods Phys. Res., Sect. A **193**, 415 (1982).
- [13] K.-J. Kim, Phys. Rev. Lett. **57**, 1871 (1986).
- [14] R. Bonifacio *et al.*, Riv. Nuovo Cimento **13**, 9 (1990).
- [15] J. Gardelle, J. Labrouche, and J.L. Rullier, Phys. Rev. Lett. **76**, 4532 (1996); J. Gardelle *et al.*, Phys. Plasmas **3**, 4197 (1996).
- [16] J. Gardelle *et al.*, Phys. Rev. Lett. **79**, 3905 (1997).
- [17] J. Bardy *et al.*, Nucl. Instrum. Methods Phys. Res., Sect. A **304**, 311 (1991).
- [18] J. Gardelle *et al.*, Phys. Rev. E **50**, 4973 (1994).
- [19] W. Barletta *et al.*, Nucl. Instrum. Methods Phys. Res., Sect. A **329**, 348 (1993).
- [20] N. Piovella *et al.*, Phys. Rev. Lett. **72**, 88 (1994).